Elsevier Editorial System(tm) for Journal of Controlled Release

Manuscript Draft

Manuscript Number:

Title: Pin1 liposomal inhibitor is an effective therapy in high-grade serous ovarian cancer

Article Type: Research paper

Keywords: Pin1, ovarian cancer, liposome, nanomedicine, nanotechnology, small molecule inhibitors.

Corresponding Author: Dr. flavio rizzolio, PhD

Corresponding Author's Institution: Centro di Riferimento Oncologico

First Author: Concetta Russo Spena

Order of Authors: Concetta Russo Spena; Lucia De Stefano; Stefano Palazzolo; Barbara Salis; Carlotta Granchi; Filippo Minutolo; Tiziano Tuccinardi; Robert Fratamico; Sara Crotti; Sara D'Aronco; Marco Agostini; Giuseppe Corona; Isabella Caligiuri; Vincenzo Canzonieri; Flavio Rizzolio, Researchr

Abstract: Pin1, a prolyl isomerase that sustains tumor progression is overexpressed in different types of cancers. Functional inactivation of Pin1 restrains tumor growth and leaves normal cells unaffected making it an ideal pharmaceutical target. Although many studies focused on hormonal cancers, ovarian cancer is under investigated. Here, we show that Pin1 is an important therapeutic target in high-grade serous ovarian cancers. Knock down of Pin1 in ovarian cancer cell lines induces apoptosis and restrains tumor growth in a syngeneic mouse model. Since specific and non-covalent Pin1 inhibitors are still limited, the first liposomal formulation of a Pin1 inhibitor was designed. The drug was efficiently encapsulated in modified cyclodextrins and remotely loaded into pegylated liposomes. This liposomal formulation accumulates preferentially in the tumor and has a desirable pharmacokinetics profile. The liposomal inhibitor was able to alter Pin1 cancer driving-pathways trough the induction of proteasome-dependent degradation of Pin1 and in vivo it resulted effective to curb ovarian tumor growth in vivo.

Suggested Reviewers: Twan Lammers Chemist
Professor, Dept. of Cancer diagnosis and therapy, Utrecht University
tlammers@ukaachen.de
Expert in nanomedicine and drug delivery applications

Anil Kumar Chemist
Professor, Chemistry, Institute of technology Roorkee, India
anilkfcy@iitr.ac.in
Expert on the synthesis of nanomaterials

Pietro Traldi Chemist
Researcher, IENI - CNR, Padua
pietro.traldi@adr.pd.cnr.it
Expert of mass spectrometry

Marco Lucio Lolli Chemist
Researcher, Pharmacy, University of Torino
marco.lolli@unito.it
Expert in Medicinal chemistry and Pin1

Maurizio Giannì Biologist
Researcher, Biochemistry and Molecular Pharmacology, Mario Negri of Milano
maurizio.gianni@marionegri.it
Expert in cancer biology and Pin1

Roberto Giovannoni Biotechnologist
Researcher, School of medicine and surgery, University of Milano
roberto.giovannoni@unimib.it
Expert in oncology

Piergiorgio Percipalle Biologist
Professor, Biology, New York University
pp69@nyu.edu
Expert in cell molecular and cellular biology

*Graphical Abstract

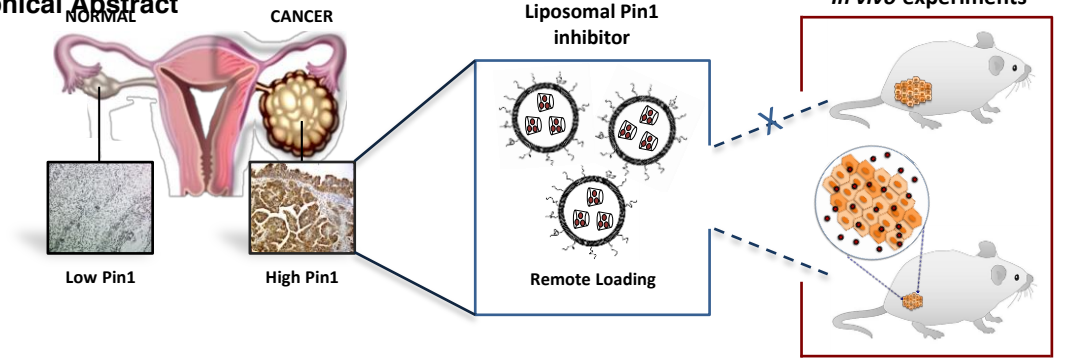

*Original Manuscript - include embeded figures/tables
Click here to view linked References

Pin1 liposomal inhibitor is an effective therapy in high-grade serous ovarian cancer

Concetta Russo Spena[1,2], Lucia De Stefano[1,2], Stefano Palazzolo[1], Barbara Salis[1,3], Carlotta Granchi[4], Filippo Minutolo[4], Tiziano Tuccinardi[4], Robert Fratamico[5], Sara Crotti[6], Sara D'Aronco[6], Marco Agostini[6,7], Giuseppe Corona[1], Isabella Caligiuri[8], Vincenzo Canzonieri[8] and Flavio Rizzolio[1,9]

1. Experimental and Clinical Pharmacology, Department of Translational Research, National Cancer Institute and Center for Molecular Biomedicine - CRO, Aviano. Italy.

2. Doctoral School in Chemistry, University of Trieste, Italy.

3. Doctoral School in Molecular Biomedicine, University of Trieste, Italy.

4. Department of Pharmacy, University of Pisa, Pisa, Italy

5. Department of Medical Oncology, Sidney Kimmel Cancer Center, Thomas Jefferson University, Philadelphia, PA

6. Institute of Pediatric Research-Città della Speranza, Padova, Italy.

7. First Surgical Clinic Section, Department of Surgical, Oncological and Gastroenterological Sciences, University of Padova, Italy.

8. Pathology Unit, Department of Molecular Biology and Translational Research, National Cancer Institute and Center for Molecular Biomedicine - CRO, Aviano, Italy.

9. Department of Molecular Sciences and Nanosystems, Ca' Foscari University, Venezia-Mestre, Italy.

Keywords: Pin1, ovarian cancer, liposome, inhibitory small molecules.

ABSTRACT

Pin1, a prolyl isomerase that sustains tumor progression, is overexpressed in different types of malignancies. Functional inactivation of Pin1 restrains tumor growth and leaves normal cells unaffected making it an ideal pharmaceutical target. Although many studies on Pin1 have focused on malignancies that are influenced by sex hormones, ovarian cancer has lagged behind. Here, we show that Pin1 is an important therapeutic target in high-grade serous ovarian cancers. Knock down of Pin1 in ovarian cancer cell lines induces apoptosis and restrains tumor growth in a syngeneic mouse model. Since specific and non-covalent Pin1 inhibitors are still limited, the first liposomal formulation of a Pin1 inhibitor was designed. The drug was efficiently encapsulated in modified cyclodextrins and remotely loaded into pegylated liposomes. This liposomal formulation accumulates preferentially in the tumor and has a desirable pharmacokinetic profile. The liposomal inhibitor was able to alter Pin1 cancer driving-pathways trough the induction of proteasome-dependent degradation of Pin1 and it was found to be effective in curbing ovarian tumor growth *in vivo*.

INTRODUCTION

High-grade serous epithelial ovarian cancer (HGSOC) is a deadly disease, which accounts for more than 150.000 deaths each year worldwide [1]. For decades, HGSOC has shown little improvement in overall survival and cytoreductive surgery followed by platinum-based chemotherapy remains the backbone of treatment [2–6]. Although most patients respond to platinum based therapy, the majority relapse and few effective therapies exist for this scenario [7–12]. Lack of knowledge of tumor origin was the major limitation for the discovery of new therapeutic opportunities. Only recently, new mouse models have clarified that secretory epithelial cells of the distal fallopian tube (FTSECs) are the likely progenitors of a substantial proportion of HGSOCs [13–17]. In addition, the progress in molecular characterization of tumors derived directly from patients have defined important pathways which drive HGSOCs [18,19]. Alteration of homologous recombination, PI3K/RAS, RB, NOTCH, and FOXM1 pathways are commonly seen [18].

A fundamental mechanism to control key proteins in these pathways is the phosphorylation of the proline (Pro)- Ser/Thr motifs, which are controlled by the Peptidyl-prolyl cis-trans isomerase NIMA-interacting 1 (Pin1), a unique Peptidyl-prolyl isomerases (PPIase) [20,21]. Pin1 accelerates the conversion of cis and trans isomers, which is slowed down by phosphorylation. The net result on cancer cells is the activation of oncogenes and inactivation of tumor suppressor genes [22–30]; therefore, its inhibition represents an exciting therapeutic opportunity for the treatment of HGSOCs. In addition, Pin1 possesses many unique features, which are attractive as therapeutic target: a) the PPIase domain has a specific, structurally-organized shaped active site that is suitable for drug development [31]; b) mice knocked down (KD) for Pin1 are viable without gross abnormalities [32] and c) genetic manipulation of Pin1 in several oncogene-induced mouse models of tumorigenesis limits tumor burden and metastatic spread [33]. Pin1 is expressed at low levels in

normal tissues and specifically upregulated in cancer cells and cancer stem cells, a subclass of neoplastic cells found in most tumors which are more resistant to multiple commonly used chemotherapeutic treatments [34]. Furthermore, inhibition of Pin1 sensitizes cancer cells to targeted- and chemo-therapies and reverse drug resistance [35,36]. Many research groups and companies are developing Pin1 ligands; however, in spite of highly specific molecular inhibition, they lack demonstrated effective inhibition of Pin1 and antitumor activity *in vivo*. In turn, no clinical trials have been performed due to inadequate pharmacological parameters of the developed inhibitors such as potency, solubility, and cell permeability [37]. Only recently, a specific Pin1 inhibitor possessing an *in vivo* activity has been demonstrated, albeit with a covalent mechanism of action [38].

A current approach in improving drug properties is the development of nanoparticles for drug delivery [39]. Nanodrugs retain many properties that are fundamental in cancer therapy among others: specific accumulation in the tumor taking advantage of enhanced permeability and retention (EPR) effect [40]; increased therapeutic ratio (high effectiveness and low toxicity) and improved drug solubility. Although thousands of nanomaterials are under investigation, liposomes, a bilayer of lipids that mimic the cell membrane are of great interest. Other than biocompatibility, these nanomaterials have already been approved by the Food and Drug Administration in the United States and the European Medicines Agency in Europe [41,42].

Here we demonstrated that Pin1 is overexpressed in ovarian cancer tissue samples and when knocked down, it promotes ovarian cancer cell death *in vitro* and *in vivo* demonstrating its potential as pharmacological cancer target for HGSOC. For the first time, we encapsulated a selective Pin1 inhibitor designed by Pfizer into liposomes [43]. Utilizing a similar method developed by Vogelstein's group [44], we successfully loaded the drug/modified cyclodextrin

complex by remote loading into liposomes and utilized it to kill ovarian cancer cells in an *in vivo* model.

2. Experimental section

2.1 Cell culture treatment and reagents

OVCAR3, MRC-5, T47D, PLC/PRF/5 and NIH-3T3 cell lines were purchased from ATCC and grown as indicated. Kuramochi, Ovsaho and COV318 cell lines were generously provided by Gustavo Baldassarre and grown in RPMI and DMEM media with 10% FBS, respectively. STOSE cell lines were generously provided by Barbara Vanderhyden and grown in DMEM media with 4% FBS.

T47D and PLC/PRF/5 were seeded with a density of $5X10^5$ in 100 X 20 mm tissue culture dish (Falcon® Corning Brand) one day before treatment. The cells were treated with liposomal/cyclodextrin/compound **8** (LC8) 100 μM and with ATRA 10 μM for 24h then the cells were collected for western blot analysis.

$3x10^5$ NIH3T3 cells were plated one day before treatment. Cells were treated with 0, 50 and 100 μM of LC8, collected after 48h and analyzed by RT-PCR or cells were treated with 100 μM of LC8 and DMSO as control for 24h followed by 10μg/mL of CHX. Cells were collected after 0, 3, 6, 12 and 24h for western blot analysis. Cells were also treated with 0, 50 and 100 μM of LC8 for 48h and then treated with MG132 10 μM and after 6h collected for western blot analysis.

Pin1 knock down experiments were performed as previously described [26]. Human KD1 (TRCN0000001033), KD2 (TRCN0000010577) and mouse KD1 (TRCN0000012580), KD2 (TRCN0000012582) were purchased from Sigma-Aldrich (St. Louis, Mo, US).

Oligonucleotides were purchased from IDT technology (Coralville, IA, US): m/hPin1-f: 5-CAAGGAGGAGGCCCTGGAGC; m/h Pin1-r: 5-TGCATCTGACCTCTGCTGAAGG; mHPRT-f: 5-AGTACTTCAGGGATTTGAATCACG; mHPRT-r 5-GGACTCCTCGTATTTGCAGATTC; β act-Fw: 5-GACCCAGATCATGTTTGAGA; β act-rev: GACTCCATGCCCAGGAAG

Antibodies utilized in western blot experiments: mouse Cyclin D1 1:1000 (556470; BD Pharmigen^{TM}, Franklin Lakes, NJ, USA); rabbit β-catenin 1:1000 (#8480S) and rabbit anti β-actin 1:1000 (#4967S) from Cell Signaling Technology, Danvers, MA, US; rabbit LC3B 1:1000 (GTX127375; GeneTex, Irvine, CA, US); rabbit Pin1 1:250 (sc-15340), mouse Pin1 1:250 (sc-46660) and mouse Hsp70 1:1000 (sc-24) from Santa Cruz, CA, US. Secondary antibodies were from Thermo Fisher Scientific, MA, US: anti-rabbit (31464, 1:5000) and anti-mouse (31432, 1:5000).

Ultra-grade acetonitrile and formic acid (>98 %) were purchased from Romil LTD (Cambridge, UK). Filtered, deionized water was purified using a Milli-Q Academic/Quantum EX system (Millipore, Milford, MA, USA).

2.2 Immunohistochemical analysis

OV2001 and OV802 were purchased from US Biomax Inc. (Rockville, MD) and analyzed by immunohistochemistry using PIN1 antibody (sc-15340), diluted 1:50. The antibody was incubated 1h at room temperature utilizing the ultraview DAB detection kit with CC1 buffer for 36 min in the Benchmark ultra instrument (Ventana Medical Systems, AZ, US). The tissues were analyzed with light microscopy using 10 and 20 X magnifications. The IHC staining was converted to an H score: intensity (0, 1, 2, 3) x area (0-100%). From 0 to 75 (first quartile) was defined as low expression; > 75 was defined as medium-high.

2.3 Flow cytometry, caspase 3/7 and cell viability analyses

Sub G1 analysis: cells were fixed by adding ice-cold 70% ethanol while vortexing. Fixed cells were stored at 4°C for at least 2h and then washed once with PBS. Cells were stained with 10 mg/ml propidium iodide (Roche), 20 ng/ml RNase A (Roche) in PBS, and incubated at room temperature for 1h in the dark. The percentage of cells in the different phases of the cell cycle was measured by flow cytometry (Becton-Dickinson, Franklin Lakes, NJ, USA) and analyzed with ModFit LTV4.0.5(Win) software.

Annexin V analysis was performed using a PE-Annexin V Apoptosis Detection Kit (Becton-Dickinson, Franklin Lakes, NJ, USA) according to the manufacturer's protocol. Cells were stained with PE Annexin V and 7-AAD and incubated for 30 min at room temperature (25°C) in the dark. Three-hundred µl of 1X binding buffer was added to each tube. Samples were evaluated by FACS Canto II (Becton-Dickinson, Franklin Lakes, NJ, USA) instrument within 1 h and analyzed with BD FACS DIVA software.

Caspase 3/7 assay: $1x10^5$ cells were lysed in 10 µl of NP-40 lysis buffer (0.01M Tris-HCl, 0.01M NaCl, 0.003M MgCl2, 0.03M Sucrose, and 0.5% NP-40) and incubated with 10 µl of caspase 3/7 Glo assay (Promega, Madison, WI, USA) for 1h at room temperature. Luminescence was read in a F200 Tecan instrument (Tecan, Switzerland).

Cell viability: the cells were infected with three different plasmids: two knock down and a control. Three days after infection the cells were seeded in 96-well plates (Flacon BD, San Jose, CA, US) at a density of 10^3 cells/well. The viability was evaluated by CellTiter-Glo®luminescence assay (Promega, Madison, WI, US) after 96h using an Infinite 200 PRO instrument (Tecan, Switzerland). Averages and standard deviations were obtained from triplicates.

2.4 RT-PCR, Real-time PCR and western blot analyses

Reverse transcription: Total RNA was prepared from cells using the Smarter Nucleic Acid Sample Preparation kit (Stratec biomedical, Germany). Total RNA (400 ng) was reverse transcribed in a 10 µl reaction using Go-Script RT System kit (Promega). 4 ng of cDNA were used to amplify target genes.

Semi-quantitative PCR: cDNA was amplified using GoTaq® G2 Polymerase and Master Mix (Promega, Madison, WI, US). Hprt was used as a control. PCR reactions were carried out in a final volume of 20 µL as described in the manufacturer's protocol. The PCR cycles were as follow: 5 min at 95 °C; 20 s at 95 °C, 30 s at 60 °C, 30 s at 72 °C x 30 cycles. The products were analyzed via 3% agarose gel electrophoresis.

Real-time PCR: qRT-PCR was performed with Go Taq qPCR Mastermix (Promega, Madison, Wisconsin, US) using a 7500 Real Time PCR System instrument (Applied Biosystems, Foster City, CA, US). Samples were run in duplicates and all the values were normalized to β-Actin.

Western blot analysis: Total cell extracts were obtained by treating cells with RIPA buffer 0.1% SDS plus protease and phosphatase inhibitors (Complete-EDTA, Roche, Switzerland) then incubate on ice for 20 min and sonicated for 5 s. After centrifuging at 12000 rpm for 20 min at 4 °C, equal amount of protein (50 µg) was separated by TruePage Precast Gels 4-12 % SDS-PAGE (Sigma-Aldrich Merck, Germany). Proteins were transferred onto nitrocellulose membranes (Amersham TM Protran TM 0.45□m NC from GE Healthcare Life Science), then blocked for 30 min with 5% non fat dried milk in TBS containing 0,1% Tween 20 (TBS-T). The membranes were incubated with primary antibodies at 4° C ON, washed three times with TBS-Tween and incubated with HRP-conjugated secondary antibodies for 1h at room temperature. The results were visualized by ECL western blot analysis detection system.

*2.5 Synthesis of compound **8***

A representative Pin1 inhibitor (compound **8**, Scheme S1; compound 17 in Guo *et al*., [43]), belonging to the alkyl amide indole-based library of compounds developed by Pfizer was synthesized in our laboratory following the previously reported procedure [43] (see Supplemental methods).

2.6 Liposomal formulation

Pegylated liposomes: 1,2-distearoyl-*sn*-glycero-3-phosphocholine (DSPC), cholesterol, and 1,2-dipalmitoyl-*sn*-glycero-3-phosphoethanolamine-N-[methoxy(polyethylene glycol)-2000 (DPPE-PEG) from Avanti Polar Lipids (50:45:5, molar ratio) were dissolved in chloroform (20 mL). The solvent was removed by vacuum to form a thin lipid film, which was hydrated by shaking in the appropriate buffer (80 mM Arg·Hepes, pH 9.0) at 65 °C for 2 h. The vesicle suspension was serially extruded through 0.4-, 0.2- and 0.1- μm polycarbonate membranes (Whatman; Nuclepore Track- Etched Membrane) at 65°C to obtain mono-dispersed liposomes. A transmembrane gradient was created by an ON dialysis in PBS. The average size and polydispersity index were measured by dynamic light scattering experiments on a Zetasizer Nano ZSP (ZEN 5600-Malvern Instruments, Malvern, UK).

Cyclodextrin-Inhibitor (CI) complex: compound **8** was dissolved in methanol and mixed with equimolar quantity of Heptakis-(6- amino- 6- deoxy)- β- Cyclodextrin 7xHCl (CDexB- 013; Arachem, Netherlands) in deionized water. In detail, the methanolic solution of the drug was added in a dropwise fashion to the cyclodextrin solution in agitation (final concentration of methanol was 10%). This suspension was shaken at 55 °C for 48h. The solution was flash-frozen in a dry ice/acetone bath followed by lyophilization and then stored at −20 °C until further use.

Liposomes/cyclodextrin/compound **8** complex: After lyophilization, CI was incubated with 20mg/mL of liposomal solutions for 1h at 65 °C. The sample was spun at maximum speed in order to remove the particulate matter. The amount of inhibitor loaded within the liposomes was determined by UV-Visible method utilizing a calibration curve (NanoDrop 2000c; Thermo Fisher Scientific, Waltham, MA, US). The inhibitor and LC8 were dissolved in methanol and analyzed at 270 nm.

2.7 Loading and release

The loading of inhibitor was evaluated with the UV-VIS method using the NanoDrop 2000c instrument after disruption of the liposomal solution with methanol: 5µl of LC8 was dissolved in 600µl of methanol. The inhibitor presents a characteristic peak at 270 and 290 nm. The release of inhibitor was evaluated from dialysis membrane (Slide-A-Lyzer® MINI Dialysis Devices, 20K MWCO) at room temperature.

2.8 Half maximal inhibitory concentration (IC_{50})

In order to evaluate the IC_{50} of inhibitor and inhibitor loaded inside the liposomes (LC8), cells were plated in a 96-well plate one day before treatment (OVCAR3: 10^3 cells/well; MRC-5 10^4 cells/well). Then the cells were treated with inhibitor, LC8, and empty liposomes starting with a concentration of 100µM followed by five 1:2 serial dilutions. After 96h, the cell viability was evaluated by CellTiter-Glo® Luminescence assay (Promega, Madison, Wisconsin, US) with the Infinite 200 PRO instrument (Tecan) and IC_{50} was calculated using the GraphPad program (Prism, CA, US).

2.9 Animal studies

Animal studies were done in accordance to the Italian Governing Law (D.lgs 26/2014) under the authorization of Ministry of Health n° 788/2015-PR and performed in accordance with the institutional guidelines. Data are reported as the mean and standard error. $5x10^6$ OVCAR3 cell line were mixed with DMEM w/o phenol red/50% of Cultrex® Basement Membrane Matriz, Type 3 (Trevigen) and implanted subcutaneously into the flanks of 6-week-old female nude mice (Envigo, UK). When tumors reached a measurable size, mice were treated i.p. with LC8 one time per week for three treatments. Tumor volumes were measured with a caliper and calculated using the formula: $(length \times width^2)/2$. 10^7 STOSE cells were injected i.p. into 8-week-old female FVB/N mice (Envigo, UK).

PK: the experiment was performed in 8 weeks old FVB/N mice (Envigo, UK) treated with 20mg/kg (i.p.) of the drug diluted in PBS 1X. A hundred µl of blood was collected after 0.16, 3, 6, 12 and 24h and analyzed by liquid chromatography tandem mass spectrometry (LC-MS/MS).

Biodistribution: female nude mice (Envigo, UK) were treated at a dose of 20mg/kg and sacrificed after 72h. The organs were washed with 10ml of cold PBS/heparin before collection, diluted in 500 µl of PBS/BSA 4%, and homogenized with Qiagen Tissue Ruptor for 20 s at power 4 in ice. Samples were stored at -80 °C. The concentrations of inhibitor were measured by LC-MS/MS.

2.10 LC-MS/MS

Before extraction, a known amount of internal standard (IS) solution (Guo *et al*., [43], compound 16) was added to PK and biodistribution samples. Then, acetonitrile/0.1 % formic acid was added (final volume ratio, 1:2); samples were vortexed and placed into a sonicator bath for 5 min at 4° C. This procedure was performed twice and after centrifugation (14000 rpm, 20 min, 4° C), supernatants were collected together and dried under vacuum (Univapo 150 H). Calculated

extraction recoveries are reported in Table S1. Five-point calibration curves within the analyte concentration ranges 0.6–2857.1 ng/ml and 0.2–95 ng/ml were prepared in blank serum and tissue samples, obtained from untreated mice.

LC-MS/MS analysis was performed with an UltiMate 3000 system (ThermoFisher Scientific, CA, USA) coupled to an API 4000 triple quadrupole mass spectrometer (AB SCIEX, Massachusetts, USA) working in multiple reaction monitoring (MRM) modality. Selected transitions for Compound **8** and IS were as follows: m/z 423.1 > 206.1 and m/z 423.1 > 218.1 for Compound **8**; m/z 391.1 > 206.2 and m/z 391.1 > 188.1 for IS. The optimized ESI (+) source parameters are reported in Table S1. Chromatographic separation was performed on a Hypersil GOLD C8 column (2.1 × 100 mm, 3 µm, ThermoFisher Scientific). Elution was achieved by a linear gradient (mobile phase A: 0.1 % formic acid, mobile phase B: acetonitrile/0.1 % formic acid) from 30 % to 95 % B over 4 min. Injection volume was 10µl and flow rate was 300µl/min.

2.11 Statistical analysis

The statistical significance was determined using the two-tails paired t-test, unless specified. A p-value less than 0.05 was considered significant for all comparisons done.

3. Results and discussion

3.1 Pin1 expression is altered in serous ovarian cancer patients

Pin1 controls many oncogenes and tumor suppressor genes and for this reason is of wide interest as a therapeutic target. The majority of studies focused on limited tumor types, including breast and prostate [45,46]. In contrast no published works in the literature deeply investigate Pin1 in ovarian cancer. As a first step, we took advantage of the whole genome data released from The Cancer Genome Atlas (TCGA) consortium. The data were filtered for the presence of multiple alterations (amplification, deletion and mutation) in different tumor types. Fig. S1 showed that Pin1 is mostly altered in hormonal cancers with HGSOC in the top position.

In support of the genomic amplification of Pin1, it has been reported to be frequently increased at the protein level in different types of cancers [47–52] and it is a good prognostic factor in hormone-dependent tumors [23,46]. A few analyses focused specifically on ovarian cancer [53]. To strength these data, we have analyzed by immunohistochemistry (IHC) 180 cases of serous ovarian cancer on tissue microarray (TMA). Among these, 59.4% were grade 3. The expression values were divided into two categories: low and medium-high (see Experimental section). In Fig. 1a, an example of these categories was reported. When compared to adjacent normal tissue (13 cases), Pin1 is significantly upregulated (p-value 0.0012, Fisher exact test) (Fig. 1b). Taken our data and the results from the TCGA into consideration, we concluded that Pin1 deserved further investigation as potential therapeutic target in ovarian cancer.

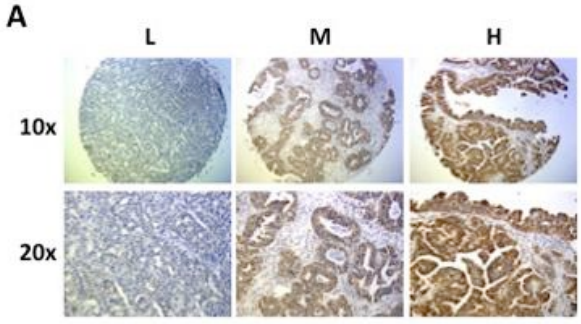

B

	Pin1		
	Low	Mid-High	Total
Serous	**77** (42.8%)	**90** (50%)	**167** (92.8%)
Normal	**12** (6.7%)	**1** (0.5%)	**13** (7.2%)
Total	**89** (49.4%)	**91** (50.6%)	**180** (100%)
p_value	**0.0012**		

Fig. 1. *Pin1 is highly expressed in HGSOC. (A) Representative images of Pin1 categorized as low, medium and high expression at different magnifications. (B) Pin1 protein is upregulated in cancer vs normal tissues. Fifty percent of cancer tissues have medium-high expression of Pin1 compared to 0.5% in normal tissues (Fisher's exact test).*

3.2 Pin1 knock down restrains tumor growth in a syngeneic ovarian tumor model

To understand if Pin1 is a valid therapeutic target in HGSOC, we knocked down its expression in different ovarian cancer cell lines that recently have been demonstrated to closely represent ovarian cancer patients [54–56]. The knock down experiments were evaluated at RNA and protein levels. Fig. S2 shows that both human and mouse shRNAs efficiently down regulate the expression of Pin1. Pin1 activity was evaluated in a spontaneously transformed mouse ovarian surface epithelial cancer cell line (STOSE), which closely recapitulates the characteristics of human HGSOC [57]. Pin1 knock down cells were less viable than normal cells and its upregulation increases cell viability (two side t-test, p-value < 0.05), (Fig. 2A). Since STOSE cell lines derived from FVB/N mice (syngeneic), normal and knock down cells were injected

intraperitoneally (i.p.). Fig. 2B demonstrates that Pin1 KD abolishes tumor formation after >3 months of follow up.

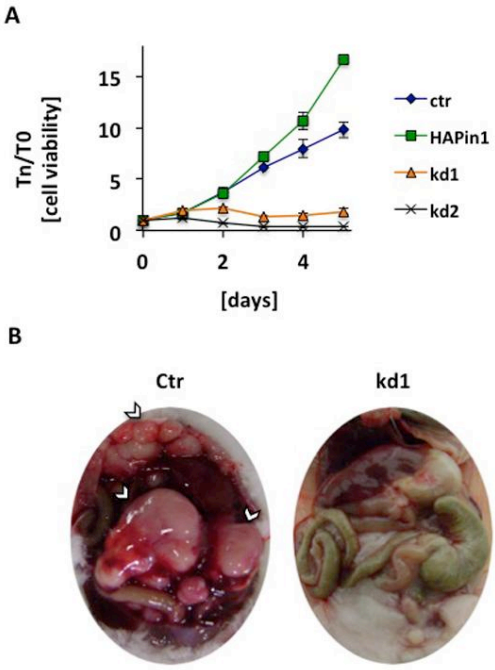

Fig.2*. Pin1 knock down reduces tumor growth in vitro and in a syngeneic model of HGSOC. (A) Cell viability of STOSE cells (Pin1 wt, kd and overexpress) were monitored for 5 days. Values on y-axis are normalized to day 0. (B) Representative images of FVB/N mice injected i.p. with STOSE cells wild type or kd for Pin1 (n=3).*

3.3 Pin1 induces cell death in human HGSOC cell lines

The population of sub-G1 cells was evaluated in Pin1 KD human cell lines. Kuramochi, COV318, and OVCAR3 cell lines showed an increase in sub-G1 phase when Pin1 was knocked down (two side t-test, p-value < 0.05), (Fig. 3A). To discriminate if a real apoptosis program was activated, cells were analyzed for Annexin V staining. Fig. 3B,C demonstrates that knock down cells have an increased number of apoptotic cells (early and total apoptosis) compared to normal cells (two side t-test, p-value < 0.05). To gain insight into the molecular mechanism that leads to

apoptosis, caspase 3/7 were evaluated. The activity of these protease enzymes increases in knock down cells (two side t-test, p-value < 0.05), (Fig. 3D).

In conclusion, the results obtained from human and mouse HGSOC models confirmed that Pin1 is a valid therapeutic target for HGSOC patients.

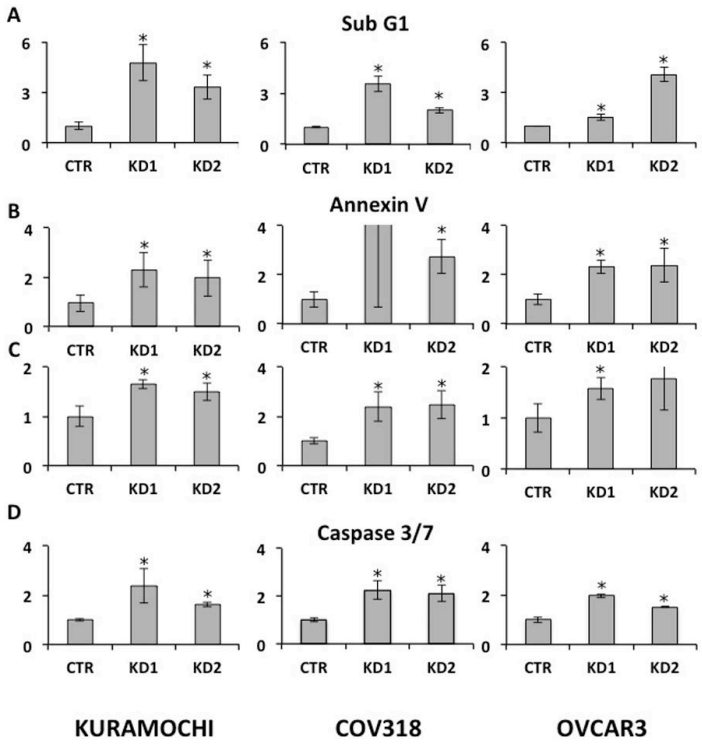

Fig. 3. *Pin1 knock down induces apoptosis in ovarian cancer cell lines. Pin1 was kd in Kuramochi, COV318, and Ovcar3 cell lines. (A) Sub G1 was determined by propidium iodide staining (≥ three independent experiments). (B) Early and (C) total apoptosis were determined by Annexin V/7-AAd staining (≥ three independent experiments). (D) Activation of caspase 3/7 was analyzed on cell extracts by luminescence (Caspase-Glo® 3/7 Assay Systems, Promega) (≥ two independent experiments). All the values on y-axis are normalized to the control. (*, p value < 0.05).*

3.4 Liposomal/cyclodextrin/compound8 (LC8) has desired pharmacological properties

Liposomal nanoparticles have been successful utilized as treatments for different diseases [58]. The major advantages are biocompatibility and an improved therapeutic window [59]. Unfortunately, only weakly acidic or basic drugs could be stably incorporated inside the cores of liposomes [60]. Recently, the Vogelstein group demonstrated that a hydrophobic drug could be solubilized in physiologic buffers and remote loaded into liposomes by modified cyclodextrins that have the properties of weak bases or acids [44].

A representative Pin1 inhibitor (compound **8**, scheme S1), belonging to the alkyl amide indole-based library of compounds developed by Pfizer, was synthesized in our laboratory, since it was among the most potent inhibitors of the isolated enzyme, showing a *Ki* value of 75 nM. This compound could be easily synthesized but it has a low solubility profile in water and is ineffective on cancer cells [43,61,62]. Compound **8** was solubilized in Heptakis (6-amino-6-deoxy)-beta-cyclodextrins and loaded into pegylated-liposomes (see Experimental section for details). Compound **8** has a solubility of 0.30± 0.05 mg/ml. When formulated as a liposomal/cyclodextrin complex, the solubility of the Pin1 inhibitor increased by about 6 times (1.82±0.10 mg/ml) (Fig. 4A). The loading efficiency of LC8 evaluated by UV absorbance was of 91.2±5.0 percent (expressed as loaded /total drug ratio) (Fig. 4B). The hydrodynamic size of liposomes under different temperatures was determined by DLS. The size increased from 25 to 37 °C and remained stable up to 65 °C (Fig. S3). The measures pre and post loading showed a low polydispersity index with the size of liposomes that increase from 151.8±0.10 nm (pre) to 177±0.11 nm (post) (Fig. 4C). The ability of LC8 to retain compound **8** was then tested. Fig. 4D demonstrates that the release from a semipermeable membrane of LC8 was slower than inhibitor alone. The accumulation of compound **8** into the liposome and the slow release rate may contribute to the change in the *in vivo* pharmacological properties. As proof of concept, LC8 was tested on OVCAR3 cells. Although compound **8** has no activity, LC8 has an IC_{50} value in the

low micromolar range (Fig. 4E). LC8 has no activity on MRC-5 normal fibroblasts (data not shown). These results allowed us to test LC8 in an *in vivo* mouse model.

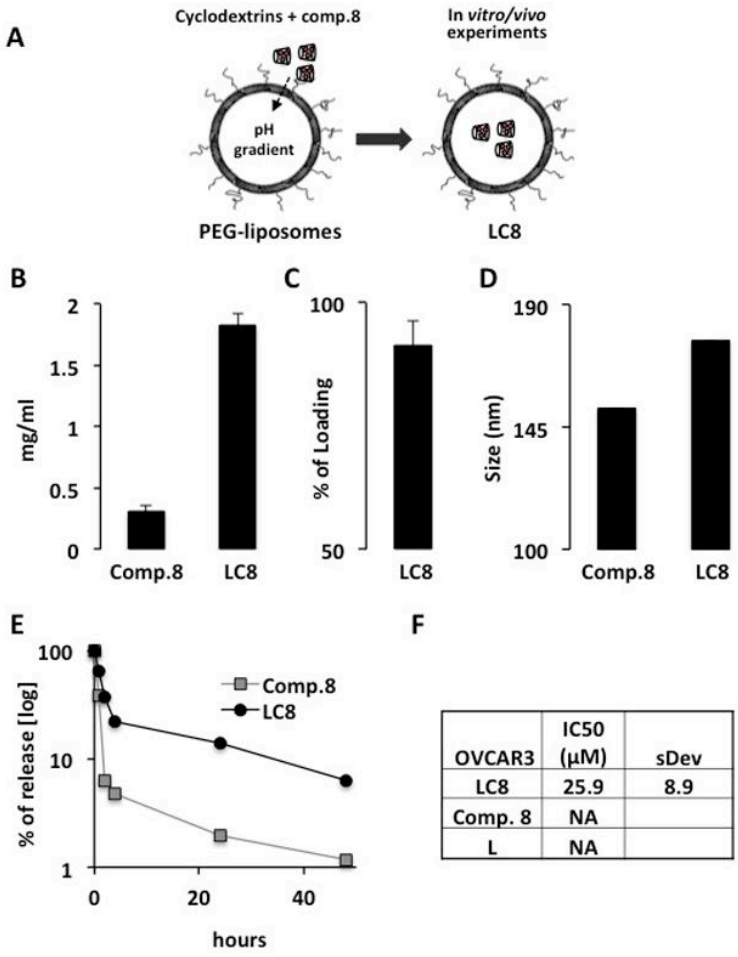

Fig. 4. *Liposomal/cyclodextrin/compund8 (LC8) is effective on OVCAR3 cell line. (A) Schematic representation of the active loading of compound 8 (Comp.8) into pegylated liposomes. (B) LC8 increases the solubility of comp. 8 in PBS solution by about 6 times. (C) The loading efficiency of comp. 8 into pegylated liposomes is more than 90%. (D) DLS analysis of liposomes before (L) and after loading of LC8. (E) Release of comp. 8 or LC8 through a semipermeable membrane. (F) OVCAR3 cell line was treated with comp. 8, LC8 or empty liposomes (L) and the IC50 was determined after 96 hours.*

3.5 LC8 promotes Pin1 protein degradation

High affinity or covalent inhibitors promote degradation of Pin1 [38,63]. To assess the effect of LC8, fibroblast cells were treated with 100 μM of LC8. We observed that LC8 caused a decrease in the level of the Pin1 protein (Fig. 5A). At the mRNA level, the treatment did not substantially alter Pin1 (Fig. 5B). To discriminate between protein degradation or decreased stability, cells were treated with MG132 (proteasome inhibitor) (Fig. 5A) or CHX (protein synthesis inhibitor) (Fig. 5C). Only MG132 rescued the expression of Pin1 confirming a specific mechanism of protein degradation mediated by the proteasome.

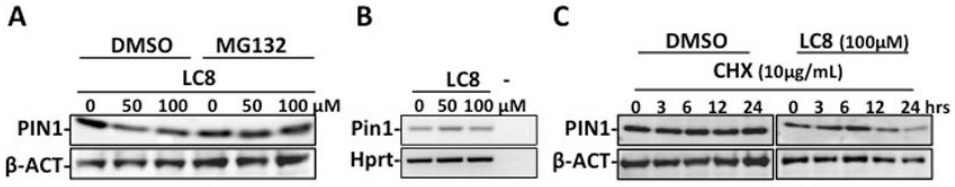

Fig. 5. *LC8 induces Pin1 degradation through the proteasome. (A) Fibroblast cells were treated with 100 μM of LC8 for 48 hours followed by 10 μM of proteasomal inhibitor MG132 for 6 hours. MG132 was abled to rescue the expression of Pin1 protein. (B) Cells were treated as in (A). Pin1 RNA levels was unaffected. (C) Fibroblast cells were treated with 100 μM of LC8 for 24 hours followed by 10 μg/ml of CHX for the indicated time. LC8 induces protein degradation through the proteasome.*

3.6 LC8 alters the levels and function of PIN1 substrates

Pin1 controls multiple cancer drive-pathways through regulation of many oncogenes and tumor suppressor genes at various levels [30]. We utilized T47D (breast) and PLC/PRF/5 (liver) cancer cell lines as published models to study LC8's effect [38,64]. Compared to untreated cells, LC8 downregulated the expression of beta-catenin, LC3B (autophagy), and cyclin D1 (cell cycle; only in T47D cells) (Fig. 6). As control we utilized ATRA, which provided similar results.

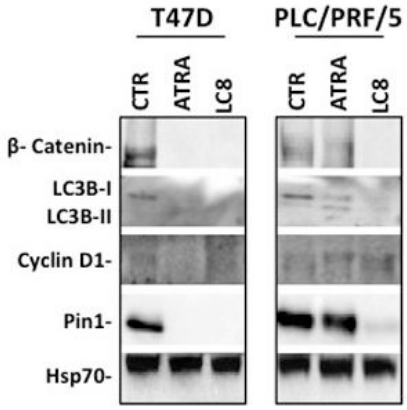

Fig. 6. *LC8 alters the expression of Pin1 target proteins. T47D and PLC/PRF/5 cell lines were treated with 10 μM of ATRA (positive control) and 100 μM of LC8 for 24 hours and analyzed by western blot. The expression of β-catenin, LC3B, and cyclin D1 was down regulated by LC8.*

3.7 LC8 is a drug for HGSOC therapy

Liposomal drugs are mostly effective *in vivo* due to their designed formulation to accumulate inside the tumor (EPR effect). Before testing the efficacy of LC8, we carried out a maximum tolerated dose (MTD) experiments. Mice were treated with a dose escalation of the liposomal formulation (without drug) and the health of the mice was monitored. We found that the mice could be treated up to 250 $mgkg^{-1}$ without evident signs of toxicity (Fig. S4A). Afterwards, the mice were treated i.p. with LC8 at the indicated doses. As an objective scale of mouse health, the body weight was followed for almost 3 months. We observed no sign of toxicity up to 40 $mgkg^{-1}$ (Fig. S4B).

OVCAR3 cells are a good model of HGSOC and can grow subcutaneously in nude mice. Cells were injected into the flanks of the mice and after tumors reached a volume of 168.2 ± 27.97, the animals were treated with 20$mgkg^{-1}$ of LC8 as in the MTD experiment. LC8 significantly decreased tumor volume compared to untreated mice (Fig. 7A). The body weight of the mice in both groups remained unchanged (Fig. 7B). Serum pharmacokinetic analysis of the drug showed

two-kinetic phases of elimination, with a major decrement in the first 10h (Fig. 7C). Interestingly, the biodistribution of LipoPin1 after 72h showed a main accumulation in the tumor followed by liver, spleen, and skin (Fig. 7D).

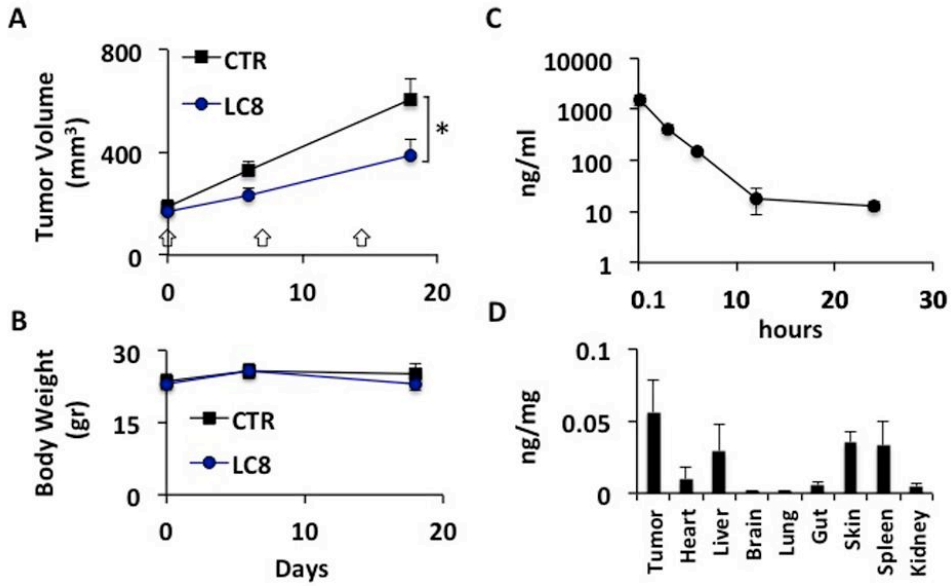

Fig. 7. *LC8 is effective in a HGSOC mouse tumor model. Nude mice were subcutaneously injected with 5x10⁶ OVCAR3 cell line (n=12) and (A) tumor volume and (B) body weight were followed for 18 days. LC8 was injected i.p. every 7 days (arrows) at a dose of 20 mg/kg. LC8 was effective to reduce tumor burden without compromising animal health. (C) FVB/N mice (n=3, data point) were i.p. injected with 20 mg/kg and plasma was analyzed at indicated time point. (D) Nude mice (n=3, data point) were i.p. injected with 20 mg/kg of LC8 and analyzed after 72h. LC8 accumulated mainly in the tumor.*

4. Conclusions

This investigation first reports the preparation of an effective liposomal formulation of a potent and selective Pin1 inhibitor. The new nanoformulation dramatically improves the *in vitro* and in *vivo* pharmacological properties of the Pin1 inhibitor. We showed that Pin1 is overexpressed in human serous ovarian cancer and its inhibition induces cell death and tumor growth reduction in a mouse metastatic immunocompetent ovarian and human subcutaneous ovarian cancer models. The development of such new active liposome formulations may pave the way for clinical experimentation and support for a new effective targeted therapy for ovarian cancer patients.

5. Funding Sources

My First AIRC (No. 1569)

6. Acknowledgments

Authors are grateful and would like to recognize the Associazione Italiana per la Ricerca sul Cancro –AIRC.

Competing interests

The authors declare no competing interests.

References

(1) Bowtell, D. D.; Böhm, S.; Ahmed, A. A.; Aspuria, P.-J.; Bast, R. C.; Beral, V.; Berek, J. S.; Birrer, M. J.; Blagden, S.; Bookman, M. A.; *et al*. Rethinking Ovarian Cancer II: Reducing Mortality from High-Grade Serous Ovarian Cancer. *Nat*. *Rev*. *Cancer* **2015**, *15*, 668–679.

(2) Mutch, D. G. Surgical Management of Ovarian Cancer. *Semin*. *Oncol*. **2002**, *29*, 3–8.

(3) Greenlee, R. T.; Hill-Harmon, M. B.; Murray, T.; Thun, M. Cancer Statistics, 2001. *CA*. *Cancer J*. *Clin*. **2001**, *51*, 15–36.

(4) Jodrell, D. I.; Egorin, M. J.; Canetta, R. M.; Langenberg, P.; Goldbloom, E. P.; Burroughs, J. N.; Goodlow, J. L.; Tan, S.; Wiltshaw, E. Relationships between Carboplatin Exposure and Tumor Response and Toxicity in Patients with Ovarian Cancer. *J*. *Clin*. *Oncol*. **1992**, *10*, 520–528.

(5) Della Pepa, C.; Tonini, G.; Pisano, C.; Di Napoli, M.; Cecere, S. C.; Tambaro, R.; Facchini, G.; Pignata, S. Ovarian Cancer Standard of Care: Are There Real Alternatives? *Chin*. *J*. *Cancer* **2015**, *34*, 17–27.

(6) Gordon, A. N.; Stringer, C. A.; Matthews, C. M.; Willis, D. L.; Nemunaitis, J. Phase I Dose Escalation of Paclitaxel in Patients with Advanced Ovarian Cancer Receiving Cisplatin: Rapid Development of Neurotoxicity Is Dose-Limiting. *J*. *Clin*. *Oncol*. **1997**, *15*, 1965–1973.

(7) Kaufman, B.; Shapira-Frommer, R.; Schmutzler, R. K.; Audeh, M. W.; Friedlander, M.; Balmaña, J.; Mitchell, G.; Fried, G.; Stemmer, S. M.; Hubert, A.; *et al*. Olaparib Monotherapy in Patients With Advanced Cancer and a Germline *BRCA1/2* Mutation. *J*.

Clin. *Oncol*. **2015**, *33*, 244–250.

(8) Fong, P. C.; Boss, D. S.; Yap, T. A.; Tutt, A.; Wu, P.; Mergui-Roelvink, M.; Mortimer, P.; Swaisland, H.; Lau, A.; O'Connor, M. J.; *et al*. Inhibition of Poly(ADP-Ribose) Polymerase in Tumors from *BRCA* Mutation Carriers. *N*. *Engl*. *J*. *Med*. **2009**, *361*, 123–134.

(9) Pujade-Lauraine, E.; Hilpert, F.; Weber, B.; Reuss, A.; Poveda, A.; Kristensen, G.; Sorio, R.; Vergote, I.; Witteveen, P.; Bamias, A.; *et al*. Bevacizumab Combined With Chemotherapy for Platinum-Resistant Recurrent Ovarian Cancer: The AURELIA Open-Label Randomized Phase III Trial. *J*. *Clin*. *Oncol*. **2014**, *32*, 1302–1308.

(10) Aghajanian, C.; Blank, S. V; Goff, B. A.; Judson, P. L.; Teneriello, M. G.; Husain, A.; Sovak, M. A.; Yi, J.; Nycum, L. R. OCEANS: A Randomized, Double-Blind, Placebo-Controlled Phase III Trial of Chemotherapy with or without Bevacizumab in Patients with Platinum-Sensitive Recurrent Epithelial Ovarian, Primary Peritoneal, or Fallopian Tube Cancer. *J*. *Clin*. *Oncol*. **2012**, *30*, 2039–2045.

(11) Perren, T. J.; Swart, A. M.; Pfisterer, J.; Ledermann, J. A.; Pujade-Lauraine, E.; Kristensen, G.; Carey, M. S.; Beale, P.; Cervantes, A.; Kurzeder, C.; *et al*. A Phase 3 Trial of Bevacizumab in Ovarian Cancer. *N*. *Engl*. *J*. *Med*. **2011**, *365*, 2484–2496.

(12) Burger, R. A.; Brady, M. F.; Bookman, M. A.; Fleming, G. F.; Monk, B. J.; Huang, H.; Mannel, R. S.; Homesley, H. D.; Fowler, J.; Greer, B. E.; *et al*. Incorporation of Bevacizumab in the Primary Treatment of Ovarian Cancer. *N*. *Engl*. *J*. *Med*. **2011**, *365*, 2473–2483.

(13) Perets, R.; Wyant, G. A.; Muto, K. W.; Bijron, J. G.; Poole, B. B.; Chin, K. T.; Chen, J. Y. H.; Ohman, A. W.; Stepule, C. D.; Kwak, S.; *et al*. Transformation of the Fallopian Tube

Secretory Epithelium Leads to High-Grade Serous Ovarian Cancer in Brca;Tp53;Pten Models. *Cancer Cell* **2013**, *24*, 751–765.

(14) Flesken-Nikitin, A.; Hwang, C.-I.; Cheng, C.-Y.; Michurina, T. V.; Enikolopov, G.; Nikitin, A. Y. Ovarian Surface Epithelium at the Junction Area Contains a Cancer-Prone Stem Cell Niche. *Nature* **2013**, *495*, 241–245.

(15) Vaughan, S.; Coward, J. I.; Bast, R. C.; Berchuck, A.; Berek, J. S.; Brenton, J. D.; Coukos, G.; Crum, C. C.; Drapkin, R.; Etemadmoghadam, D.; *et al*. Rethinking Ovarian Cancer: Recommendations for Improving Outcomes. *Nat*. *Rev*. *Cancer* **2011**, *11*, 719–725.

(16) Kim, J.; Coffey, D. M.; Creighton, C. J.; Yu, Z.; Hawkins, S. M.; Matzuk, M. M. High-Grade Serous Ovarian Cancer Arises from Fallopian Tube in a Mouse Model. *Proc*. *Natl*. *Acad*. *Sci*. **2012**, *109*, 3921–3926.

(17) Sherman-Baust, C. A.; Kuhn, E.; Valle, B. L.; Shih, I.-M.; Kurman, R. J.; Wang, T.-L.; Amano, T.; Ko, M. S.; Miyoshi, I.; Araki, Y.; *et al*. A Genetically Engineered Ovarian Cancer Mouse Model Based on Fallopian Tube Transformation Mimics Human High-Grade Serous Carcinoma Development. *J*. *Pathol*. **2014**, *233*, 228–237.

(18) Integrated Genomic Analyses of Ovarian Carcinoma. *Nature* **2011**, *474*, 609–615.

(19) Zhang, H.; Liu, T.; Zhang, Z.; Payne, S. H.; Zhang, B.; McDermott, J. E.; Zhou, J.-Y.; Petyuk, V. A.; Chen, L.; Ray, D.; *et al*. Integrated Proteogenomic Characterization of Human High-Grade Serous Ovarian Cancer. *Cell* **2016**, *166*, 755–765.

(20) Yaffe, M. B.; Schutkowski, M.; Shen, M.; Zhou, X. Z.; Stukenberg, P. T.; Rahfeld, J. U.; Xu, J.; Kuang, J.; Kirschner, M. W.; Fischer, G.; *et al*. Sequence-Specific and Phosphorylation-Dependent Proline Isomerization: A Potential Mitotic Regulatory

Mechanism. *Science* **1997**, *278*, 1957–1960.

(21) Ranganathan, R.; Lu, K. P.; Hunter, T.; Noel, J. P. Structural and Functional Analysis of the Mitotic Rotamase Pin1 Suggests Substrate Recognition Is Phosphorylation Dependent. *Cell* **1997**, *89*, 875–886.

(22) Gianni, M.; Boldetti, A.; Guarnaccia, V.; Rambaldi, A.; Parrella, E.; Raska Jr., I.; Rochette-Egly, C.; Del Sal, G.; Rustighi, A.; Terao, M.; *et al*. Inhibition of the Peptidyl-Prolyl-Isomerase Pin1 Enhances the Responses of Acute Myeloid Leukemia Cells to Retinoic Acid via Stabilization of RARalpha and PML-RARalpha. *Cancer Res* **2009**, *69*, 1016–1026.

(23) Girardini, J. E.; Napoli, M.; Piazza, S.; Rustighi, A.; Marotta, C.; Radaelli, E.; Capaci, V.; Jordan, L.; Quinlan, P.; Thompson, A.; *et al*. A Pin1/mutant p53 Axis Promotes Aggressiveness in Breast Cancer. *Cancer Cell* **2011**, *20*, 79–91.

(24) Zacchi, P.; Gostissa, M.; Uchida, T.; Salvagno, C.; Avolio, F.; Volinia, S.; Ronai, Z.; Blandino, G.; Schneider, C.; Del Sal, G. The Prolyl Isomerase Pin1 Reveals a Mechanism to Control p53 Functions after Genotoxic Insults. *Nature* **2002**, *419*, 853–857.

(25) La Montagna, R.; Caligiuri, I.; Maranta, P.; Lucchetti, C.; Esposito, L.; Paggi, M. G.; Toffoli, G.; Rizzolio, F.; Giordano, A. Androgen Receptor Serine 81 Mediates Pin1 Interaction and Activity. *Cell Cycle* **2012**, *11*, 3415–3420.

(26) Rizzolio, F.; Lucchetti, C.; Caligiuri, I.; Marchesi, I.; Caputo, M.; Klein-Szanto, A. J.; Bagella, L.; Castronovo, M.; Giordano, A. Retinoblastoma Tumor-Suppressor Protein Phosphorylation and Inactivation Depend on Direct Interaction with Pin1. *Cell Death Differ* **2012**, *19*, 1152–1161.

(27) Lucchetti, C.; Caligiuri, I.; Toffoli, G.; Giordano, A.; Rizzolio, F. The Prolyl Isomerase Pin1 Acts Synergistically with CDK2 to Regulate the Basal Activity of Estrogen Receptor α in Breast Cancer. *PLoS One* **2013**, *8*, e55355.

(28) La Montagna, R.; Caligiuri, I.; Giordano, A.; Rizzolio, F. Pin1 and Nuclear Receptors: A New Language? *J*. *Cell*. *Physiol*. **2013**, *228*, 1799–1801.

(29) Rizzolio, F.; Caligiuri, I.; Lucchetti, C.; Fratamico, R.; Tomei, V.; Gallo, G.; Agelan, A.; Ferrari, G.; Toffoli, G.; Klein-Szanto, A. J.; *et al*. Dissecting Pin1 and Phospho-pRb Regulation. *J Cell Physiol* **2013**, *228*, 73–77.

(30) Zhou, X. Z.; Lu, K. P. The Isomerase PIN1 Controls Numerous Cancer-Driving Pathways and Is a Unique Drug Target. *Nat*. *Rev*. *Cancer* **2016**, *16*, 463–478.

(31) Moore, J. D.; Potter, A. Pin1 Inhibitors: Pitfalls, Progress and Cellular Pharmacology. *Bioorg*. *Med*. *Chem*. *Lett*. **2013**, *23*, 4283–4291.

(32) Liou, Y. C.; Ryo, A.; Huang, H. K.; Lu, P. J.; Bronson, R.; Fujimori, F.; Uchida, T.; Hunter, T.; Lu, K. P. Loss of Pin1 Function in the Mouse Causes Phenotypes Resembling Cyclin D1-Null Phenotypes. *Proc Natl Acad Sci U S A* **2002**, *99*, 1335–1340.

(33) Lu, Z.; Hunter, T. Prolyl Isomerase Pin1 in Cancer. *Cell Res*. **2014**, *24*, 1033–1049.

(34) Singh, A.; Settleman, J. EMT, Cancer Stem Cells and Drug Resistance: An Emerging Axis of Evil in the War on Cancer. *Oncogene* **2010**, *29*, 4741–4751.

(35) Rustighi, A.; Zannini, A.; Tiberi, L.; Sommaggio, R.; Piazza, S.; Sorrentino, G.; Nuzzo, S.; Tuscano, A.; Eterno, V.; Benvenuti, F.; *et al*. Prolyl-Isomerase Pin1 Controls Normal and Cancer Stem Cells of the Breast. *EMBO Mol*. *Med*. **2014**, *6*, 99–119.

(36) Ding, Q.; Huo, L.; Yang, J.-Y.; Xia, W.; Wei, Y.; Liao, Y.; Chang, C.-J.; Yang, Y.; Lai,

C.-C.; Lee, D.-F.; *et al*. Down-Regulation of Myeloid Cell Leukemia-1 through Inhibiting Erk/Pin 1 Pathway by Sorafenib Facilitates Chemosensitization in Breast Cancer. *Cancer Res*. **2008**, *68*, 6109–6117.

(37) A J Sinclair G Peters, and P J Farrell, I. P. EBNA-2 and EBNA-LP Cooperate to Cause G0 to G1 Transition during Immortalization of Resting Human B Lymphocytes by Epstein-Barr Virus. *EMBO J* **1994**, *13*.

(38) Campaner, E.; Rustighi, A.; Zannini, A.; Cristiani, A.; Piazza, S.; Ciani, Y.; Kalid, O.; Golan, G.; Baloglu, E.; Shacham, S.; *et al*. A Covalent PIN1 Inhibitor Selectively Targets Cancer Cells by a Dual Mechanism of Action. *Nat*. *Commun*. **2017**, *8*, 15772.

(39) Blanco, E.; Shen, H.; Ferrari, M. Principles of Nanoparticle Design for Overcoming Biological Barriers to Drug Delivery. *Nat*. *Biotechnol*. **2015**, *33*, 941–951.

(40) Matsumura, Y.; Maeda, H. A New Concept for Macromolecular Therapeutics in Cancer Chemotherapy: Mechanism of Tumoritropic Accumulation of Proteins and the Antitumor Agent Smancs. *Cancer Res*. **1986**, *46*, 6387–6392.

(41) Barenholz, Y. Doxil®--the First FDA-Approved Nano-Drug: Lessons Learned. *J*. *Control*. *Release* **2012**, *160*, 117–134.

(42) Miele, E.; Spinelli, G. P.; Miele, E.; Tomao, F.; Tomao, S. Albumin-Bound Formulation of Paclitaxel (Abraxane ABI-007) in the Treatment of Breast Cancer. *Int*. *J*. *Nanomedicine* **2009**, *4*, 99–105.

(43) Guo, C.; Hou, X.; Dong, L.; Marakovits, J.; Greasley, S.; Dagostino, E.; Ferre, R.; Catherine Johnson, M.; Humphries, P. S.; Li, H.; *et al*. Structure-Based Design of Novel Human Pin1 Inhibitors (III): Optimizing Affinity beyond the Phosphate Recognition

Pocket. *Bioorg*. *Med*. *Chem*. *Lett*. **2014**, *24*, 4187–4191.

(44) Sur, S.; Fries, A. C.; Kinzler, K. W.; Zhou, S.; Vogelstein, B. Remote Loading of Preencapsulated Drugs into Stealth Liposomes. *Proc*. *Natl*. *Acad*. *Sci*. **2014**, *111*, 2283–2288.

(45) Napoli, M.; Girardini, J. E.; Piazza, S.; Del Sal, G. Wiring the Oncogenic Circuitry: Pin1 Unleashes Mutant p53. *Oncotarget* **2011**, *2*, 654–656.

(46) Ayala, G.; Wang, D.; Wulf, G.; Frolov, A.; Li, R.; Sowadski, J.; Wheeler, T. M.; Lu, K. P.; Bao, L. The Prolyl Isomerase Pin1 Is a Novel Prognostic Marker in Human Prostate Cancer. *Cancer Res* **2003**, *63*, 6244–6251.

(47) Lam, P. B.; Burga, L. N.; Wu, B. P.; Hofstatter, E. W.; Lu, K. P.; Wulf, G. M. Prolyl Isomerase Pin1 Is Highly Expressed in Her2-Positive Breast Cancer and Regulates erbB2 Protein Stability. *Mol*. *Cancer* **2008**, *7*, 91.

(48) Leung, K.-W.; Tsai, C.-H.; Hsiao, M.; Tseng, C.-J.; Ger, L.-P.; Lee, K.-H.; Lu, P.-J. Pin1 Overexpression Is Associated with Poor Differentiation and Survival in Oral Squamous Cell Carcinoma. *Oncol*. *Rep*. **2009**, *21*, 1097–1104.

(49) Jawanjal, P.; Salhan, S.; Dhawan, I.; Tripathi, R.; Rath, G. Peptidyl-Prolyl Isomerase Pin1-Mediated Abrogation of APC-β-Catenin Interaction in Squamous Cell Carcinoma of Cervix. *Rom*. *J*. *Morphol*. *Embryol*. **2014**, *55*, 83–90.

(50) Zhou, C.-X.; Gao, Y. Aberrant Expression of Beta-Catenin, Pin1 and Cylin D1 in Salivary Adenoid Cystic Carcinoma: Relation to Tumor Proliferation and Metastasis. *Oncol*. *Rep*. **2006**, *16*, 505–511.

(51) Lin, F.-C.; Lee, Y.-C.; Goan, Y.-G.; Tsai, C.-H.; Yao, Y.-C.; Cheng, H.-C.; Lai, W.-W.;

Wang, Y.-C.; Sheu, B.-S.; Lu, P.-J. Pin1 Positively Affects Tumorigenesis of Esophageal Squamous Cell Carcinoma and Correlates with Poor Survival of Patients. *J. Biomed. Sci.* **2014**, *21*, 75.

(52) Kuramochi, J.; Arai, T.; Ikeda, S.; Kumagai, J.; Uetake, H.; Sugihara, K. High Pin1 Expression Is Associated with Tumor Progression in Colorectal Cancer. *J. Surg. Oncol.* **2006**, *94*, 155–160.

(53) Bao, L.; Kimzey, A.; Sauter, G.; Sowadski, J. M.; Lu, K. P.; Wang, D. G. Prevalent Overexpression of Prolyl Isomerase Pin1 in Human Cancers. *Am J Pathol* **2004**, *164*, 1727–1737.

(54) Domcke, S.; Sinha, R.; Levine, D. A.; Sander, C.; Schultz, N. Evaluating Cell Lines as Tumour Models by Comparison of Genomic Profiles. *Nat. Commun.* **2013**, *4*, 2126.

(55) Thu, K. L.; Papari-Zareei, M.; Stastny, V.; Song, K.; Peyton, M.; Martinez, V. D.; Zhang, Y.-A.; Castro, I. B.; Varella-Garcia, M.; Liang, H.; *et al*. A Comprehensively Characterized Cell Line Panel Highly Representative of Clinical Ovarian High-Grade Serous Carcinomas. *Oncotarget* **2017**, *8*, 50489–50499.

(56) Mitra, A. K.; Davis, D. A.; Tomar, S.; Roy, L.; Gurler, H.; Xie, J.; Lantvit, D. D.; Cardenas, H.; Fang, F.; Liu, Y.; *et al*. In Vivo Tumor Growth of High-Grade Serous Ovarian Cancer Cell Lines. *Gynecol. Oncol.* **2015**, *138*, 372–377.

(57) McCloskey, C. W.; Goldberg, R. L.; Carter, L. E.; Gamwell, L. F.; Al-Hujaily, E. M.; Collins, O.; Macdonald, E. A.; Garson, K.; Daneshmand, M.; Carmona, E.; *et al*. A New Spontaneously Transformed Syngeneic Model of High-Grade Serous Ovarian Cancer with a Tumor-Initiating Cell Population. *Front. Oncol.* **2014**, *4*, 53.

(58) Chang, H.-I.; Yeh, M.-K. Clinical Development of Liposome-Based Drugs: Formulation, Characterization, and Therapeutic Efficacy. *Int*. *J*. *Nanomedicine* **2012**, *7*, 49–60.

(59) Gabizon, A.; Shmeeda, H.; Barenholz, Y. Pharmacokinetics of Pegylated Liposomal Doxorubicin: Review of Animal and Human Studies. *Clin*. *Pharmacokinet*. **2003**, *42*, 419–436.

(60) Gubernator, J. Active Methods of Drug Loading into Liposomes: Recent Strategies for Stable Drug Entrapment and Increased *in Vivo* Activity. *Expert Opin*. *Drug Deliv*. **2011**, *8*, 565–580.

(61) Dong, L.; Marakovits, J.; Hou, X.; Guo, C.; Greasley, S.; Dagostino, E.; Ferre, R.; Johnson, M. C.; Kraynov, E.; Thomson, J.; *et al*. Structure-Based Design of Novel Human Pin1 Inhibitors (II). *Bioorg*. *Med*. *Chem*. *Lett*. **2010**, *20*, 2210–2214.

(62) Guo, C.; Hou, X.; Dong, L.; Dagostino, E.; Greasley, S.; Ferre, R.; Marakovits, J.; Johnson, M. C.; Matthews, D.; Mroczkowski, B.; *et al*. Structure-Based Design of Novel Human Pin1 Inhibitors (I). *Bioorg*. *Med*. *Chem*. *Lett*. **2009**, *19*, 5613–5616.

(63) Wei, S.; Kozono, S.; Kats, L.; Nechama, M.; Li, W.; Guarnerio, J.; Luo, M.; You, M.-H.; Yao, Y.; Kondo, A.; *et al*. Active Pin1 Is a Key Target of All-Trans Retinoic Acid in Acute Promyelocytic Leukemia and Breast Cancer. *Nat*. *Med*. **2015**, *21*, 457–466.

(64) Liao, X.-H.; Zhang, A. L.; Zheng, M.; Li, M.-Q.; Chen, C. P.; Xu, H.; Chu, Q.-S.; Yang, D.; Lu, W.; Tsai, T.-F.; *et al*. Chemical or Genetic Pin1 Inhibition Exerts Potent Anticancer Activity against Hepatocellular Carcinoma by Blocking Multiple Cancer-Driving Pathways. *Sci*. *Rep*. **2017**, *7*, 43639.

Supplementary Material-Figures

Click here to download Supplementary Material: Supplemental_Figures.docx

Supplementary Material-METHODS

Click here to download Supplementary Material: Supplemental_Methods.docx